AIP | Applied Physics Letters

0.42 TW 2-cycle pulses at 1.8 μm via hollow-core fiber compression

Vincent Cardin, Nicolas Thiré, Samuel Beaulieu, Vincent Wanie, François Légaré, and Bruno E. Schmidt

Citation: Applied Physics Letters **107**, 181101 (2015); doi: 10.1063/1.4934861
View online: http://dx.doi.org/10.1063/1.4934861
View Table of Contents: http://scitation.aip.org/content/aip/journal/apl/107/18?ver=pdfcov
Published by the AIP Publishing

0.42 TW 2-cycle pulses at 1.8 μm via hollow-core fiber compression

Vincent Cardin,[1] Nicolas Thiré,[1] Samuel Beaulieu,[1] Vincent Wanie,[1] François Légaré,[1,a)] and Bruno E. Schmidt[1,2,b)]
[1]*Institut National de la Recherche Scientifique, Centre Énergie Matériaux et Télécommunications, 1650 Boulevard Lionel-Boulet, Varennes, Quebec J3X1S2, Canada*
[2]*Few-cycle, Inc., 2890 Rue de Beaurivage, Montreal, Quebec H1L 5W5, Canada*

(Received 20 August 2015; accepted 17 October 2015; published online 2 November 2015)

By employing pulse compression with a stretched hollow-core fiber, we generated 2-cycle pulses at 1.8 μm (12 fs) carrying 5 mJ of pulse energy at 100 Hz repetition rate. This energy scaling in the mid-infrared spectral range was achieved by lowering the intensity in a loose focusing condition, thus suppressing the ionization induced losses. The correspondingly large focus was coupled into a hollow-core fiber of 1 mm inner diameter, operated with a pressure gradient to further reduce detrimental nonlinear effects. The required amount of self-phase modulation for spectral broadening was obtained over 3 m of propagation distance. © *2015 AIP Publishing LLC*.
[http://dx.doi.org/10.1063/1.4934861]

Gain narrowing in chirped pulse amplification (CPA)[1] sets limits for the achievable bandwidth of high power ultrafast laser systems operating in the multi-millijoule (mJ) regime. Although this limitation may be overcome with ultrabroadband optical parametric amplifiers (OPAs),[2–7] such lasers are not yet readily available commercially. Therefore, post-compression subsequent to multi-cycle laser systems remains the most proven way to generate high energy few-cycle pulses. At the mJ level of pulse energy, filamentation[8–11] and hollow-core fiber (HCF)[12] based propagation schemes still remain the most popular ones. Self-guided filamentation offers the advantages of wide spectral broadening and ease of operation. Although harder to implement, guided-mode propagation in a HCF is a much more universal method that produces spatially homogenous beams of high quality. With a proper waveguide, HCF propagation can be realized from the XUV[13] to the THz spectral range[14] and at very different energy levels (1 nJ[15]–10 mJ[16]), respectively. The concept is even applicable at average input power levels reaching 150 W.[17]

In this paper, the challenges of few-cycle HCF compression in the mid-infrared range are discussed in the context of upscaling the peak power towards the TW regime. An experimental route to circumvent these challenges is presented where pulses at 1.8 μm wavelength containing up to 11 mJ (100 Hz repetition rate) were coupled into a HCF without damaging the fiber. The maximum output energy after recompression to 2 cycles (12 fs) was 5 mJ.

The principal challenge of nonlinear pulse compression with HCFs is to provide sufficient nonlinearity for maximum self-phase modulation (SPM) while avoiding harmful nonlinear effects like self-focusing, ionization, or nonlinear mode coupling.[18] In this manner, a unique measurement of 5 fs, 5 mJ pulses at 800 nm wavelength has been reported.[19] When transferring this experiment to longer wavelengths, several quantities need to be reconsidered: the third order nonlinearity (n_2), the free electron contribution to the refractive index (n_e), the critical power for self-focusing (P_{cr}), and the waveguide attenuation (α). Table I summarizes their respective wavelength dependence.

The nonlinear refractive index of noble gases decreases with wavelength[20] (in argon, $n_2(1800\,\text{nm})/n_2(800\,\text{nm}) = 0.59$[21]). At first sight, a reduced n_2 holds promise to enable higher propagation intensities to reach the same nonlinear phase shift via SPM. Compensating the lower n_2 by increasing the intensity, however, causes an increased ionization rate. The ionization rate remains roughly constant as a function of wavelength in the tunneling regime, which is the case for peak intensities in excess of $10^{14}\,\text{W/cm}^2$. Yet, the contribution of free electrons to the refractive index, n_e, increases with laser frequency ω ($n_e^2 \propto \frac{\rho_e}{\omega^2}$), where ρ_e is the free electron density. Similarly, increasing n_2 by increasing the gas pressure equally leads to an increased free electron density. This means that gas pressure must be kept low, even though the higher critical power for self-focusing in the mid-infrared could support a much higher pressure before undesirable effects like nonlinear mode coupling come into play.[22,23]

On the other hand, lowering the intensity by using a large fiber aperture A (see Table I) reduces the ionization rate in the nonlinear medium as well as the attenuation α of the fundamental mode, which scales as $\frac{\lambda^2}{A^3}$. The lower intensity needs to be compensated by using a longer propagation length to yield the same spectral broadening without affecting the other parameters. This, however, requires perfectly straight waveguides, since the mode spacing becomes

TABLE I. Wavelength dependencies of critical parameters for the energy scaling of HCF post-compression systems. From left to right: nonlinear refractive index, free electron refractive index, critical power for self-focusing, and waveguide attenuation. The equation for the nonlinear index is part of the generalized Miller formulae as obtained in Ref. 20 and shows a monotonic decrease of n_2 with wavelength.

n_2	n_e	P_{cr}	α
$\frac{n_2(\lambda_1)}{n_2(\lambda_2)} = \left[\frac{n_0^2(\lambda_1)-1}{n_0^2(\lambda_2)-1}\right]^4$	$n_e \propto \sqrt{1-\frac{\rho_e q_e}{\varepsilon_0 m_e}\left(\frac{\lambda}{2\pi c}\right)^2}$	$\propto \frac{\lambda^2}{n_2}$	$\propto \frac{\lambda^2}{A^3}$

a)legare@emt.inrs.ca
b)schmidt@few-cycle.com

smaller for larger mode sizes, which increases the probability of linear mode coupling.

Conventional setups using capillary channels enclosed in stiff glass rods mounted on v-shaped grooves[12,24–27] are typically limited in length due to the fabrication processes and handling. Nagy *et al.*[28,29] demonstrated the use of a flexible HCF, mechanically stretched, and thus, enabling good straightness even at 3 m length. The stretched fiber was enclosed in a rigid metal tube with the fiber ends fixed permanently. In this letter, we report on an improved design which allows one to freely change the fiber length or diameter depending on the given experimental conditions. Furthermore, we demonstrate good mode guiding for waveguides of 1 mm inner diameter which is more than 500 times the wavelength (1.8 μm).

Figure 1(a) illustrates the HCF setup (shaded gray area) together with the high energy optical parametric amplifier (HE-OPA) line at the Advanced Laser Light Source (ALLS, Varennes, Canada). This OPA line is pumped by an 800 nm Ti:Sa laser at 100 Hz repetition rate. Its output is divided into 2 parts; 7 mJ are sent to a low-energy compressor (LEC) to pump a TOPAS (Light Conversion) which delivers up to 750 μJ, 50 fs pulses at 1.8 μm wavelength. The TOPAS output is spatially filtered (SF1) to ensure a clean and defined mode which is preserved in the subsequent amplification process. A clean spatial mode is a necessary requirement for optimum HCF performance. The larger energy fraction of 70 mJ is compressed in a high-energy compressor (HEC) delivering up to 50 mJ to the large aperture BBO crystal (type II, $22 \times 22 \times 2$ mm). This high energy OPA stage delivers up to 11 mJ pulses with 35 fs duration and is described in more detail in Ref. 30.

The HCF setup consists of three elements: a folded beam coupling telescope, the fiber, and the compression stage. Beam coupling is carried out with a reflective telescope. A $f = 2$ m concave mirror placed 105 cm before a $f = -2$ m convex mirror gives an effective focal length of 3.8 m with an $1/e^2$ focal size close to 750 μm. The focal spot, imaged with a Flea2 CCD (PointGrey) to characterize the spatial mode, is shown in the inset of Figure 3(a). A spatial filtering pinhole (SF2) with the same diameter as the fiber is installed directly in front of the fiber tip to prevent the fiber damage in case of beam drifts.

The fiber itself is a 3 m long, 1 mm inner diameter flexible HCF with a 300 μm thick fused silica (FS) cladding surrounded by a polymer layer. The fiber ends are permanently glued into small metal sleeves. These sleeves are clamped to holders (dark gray pieces in Figure 1) with three screws. This fast clamping solution allows one to change the propagation condition by using different fiber lengths or diameters, respectively. To straighten the fiber, tension is applied by translating one holder along the optical axis, as indicated by the arrow in Figure 1. On both sides, a two axis tilt mechanism ensures the correct alignment of the fiber tip with respect to the optical axis and allows to optimize the mode quality and transmission. The two fiber holders are connected to a KF vacuum tube through which the beam propagates under controlled pressurized conditions. High energy operation is usually achieved by applying pressure on the exit side while pumping continuously at the input. This pressure gradient provides the lowest amount of gas at entrance where the beam is the most intense, thus reducing ionization and self-focusing.[31] Indeed, ionization would hamper the waveguide qualities of the HCF, thus reducing transmission and stability. At maximum input energy of 11 mJ and 2-cycle operation, the argon pressure on the beam-input side was 300 mTorr. This value was adjusted to optimize the compression, and it is pointed out that further energy scaling seems feasible by using either Ne or He, but Ar was preferred due to its higher nonlinear index and lower cost.

Furthermore, we adjusted the ratio of focal beam waist ($1/e^2$ of intensity) over the fiber aperture to 0.75 instead of the theoretically required value of 0.64 for optimum mode coupling to the fundamental EH11 mode.[32–34] We empirically found that this slightly increased focal spot size leads to the best transmission at lower input energies around 1 mJ. The linear coupling losses were verified experimentally by inserting low energy pulses of 100 μJ in a 5 cm short HCF where propagation losses are negligible. The high transmission of 97% in this case confirmed the good beam quality

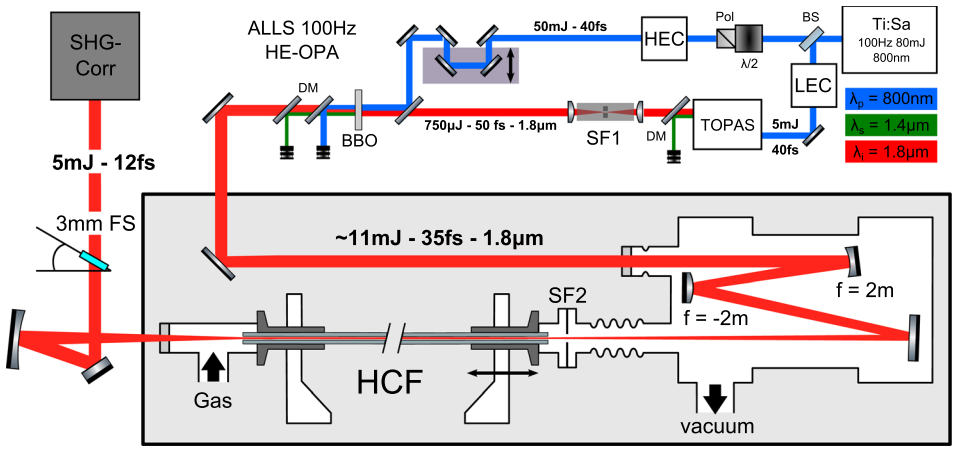

FIG. 1. Illustration of the experimental setup for the generation of high intensity few-cycle mid-infrared pulses. The top area depicts the HE-OPA of the Advanced Laser Light Source.[30] The stretched hollow-core fiber length is 3 m with 1 mm inner diameter. Depicted telescope effective focal length is 3.8 m with an $1/e^2$ beam waist of 750 μm diameter. Front vacuum chamber and exit gas inlet chamber are enclosed by 2 mm CaF_2 windows. (DM: various dichroic mirrors (as shown); Pol: Polarizer; BS: Beam splitter; LEC/HEC: Low/High Energy grating compressors; TOPAS: commercial OPA; SF: Spatial filter pinhole; SHG-Corr: all-reflective second harmonic auto-correlator.)

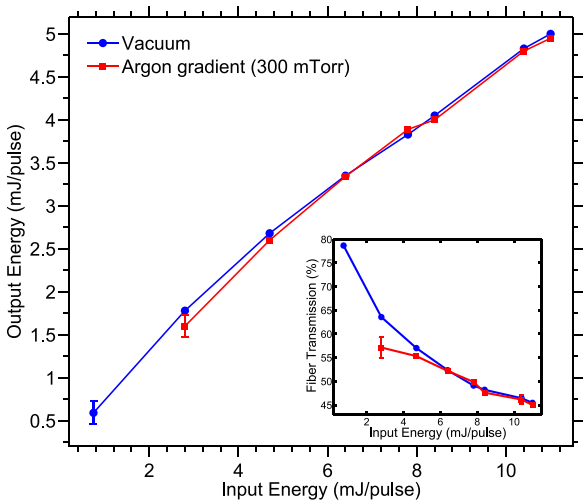

FIG. 2. Compressed output energy as a function of the fiber input energy for an evacuated (blue circles) and argon-filled (red squares) hollow-core fiber. A pressure gradient with 300 mTorr at entrance side and 520 Torr at the exit side, respectively, was applied. Inset: Corresponding transmission curve (including all vacuum windows and coupling optics) for the same data points.

achieved with the spatial filter SF1 prior to the last amplification stage and the mode matched coupling of the setup. For the 3 m long fiber, the highest transmission measured was 80% at an input energy of 750 μJ (without amplification in the last stage), which underlines the excellent guiding properties of the 3 m long HCF. The obtained output energy as a function of input energy is shown in Figure 2, with the highest output energy of 5 mJ for an input of 11 mJ. This corresponds to 45% total transmission including vacuum windows, vacuum optics, and the spatial filter SF2 in front of the fiber. The spatial beam profile subsequent to the HCF is seen in the second inset of Figure 3(a). Its $1/e^2$ diameter, after collimation at 2 m distance from the fiber output, is 7.5 mm.

Finally, 2-cycle pulse compression at 1.8 μm wavelength subsequent to the HCF was achieved by the bulk compression technique which relies on the interplay of nonlinear propagation in the fiber and linear propagation through FS subsequently.[26,27,35] By placing FS windows of correct thickness (between 2 and 4 mm), one can compress pulses close to their corresponding transform limit. The temporal characterization was performed with a second harmonic autocorrelator.

Figure 3 shows the spectral (Figure 3(a)) and temporal (Figure 3(b)) characterization of the few-cycle pulse. We achieved a spectral width spanning from 1200 nm to 2200 nm associated with a transform limited duration of 11.3 fs. The broadened spectrum in Fig. 3(a) shows the typical shape of a SPM broadened pulse with the noticeable asymmetric shape associated with self-steepening during nonlinear fiber propagation.[29,36,37] The temporal shape exhibits a Gaussian profile with a FWHM of (12.3 ± 0.4) fs corresponding to 2 cycles at 1.8 μm wavelength. A Gaussian fit is presented for comparison by the dashed lines.

To address the question about the origin for the transmission loss, we compared the throughput of an Ar filled with an evacuated fiber (40 mTorr residual pressure measured at the entrance side). Virtually no difference is observed by comparing the blue (evacuated) and red (Ar filled) curves of Figure 2 at high energy. The fact that the gas filling shows no effect on the transmission suggests an origin upstream of the fiber. Possible candidates are (i) SPM in the last BBO crystal, (ii) nonlinear effects in the vacuum window, (iii) nonlinear absorption in the dielectric mirror coatings, or (iv) beam degradation when propagating the high power mid-infrared through ambient air. Regarding the latter, we noticed a ~10% energy loss for propagation over 6–7 m of distance without any sign of self-focusing. We did, however, not observe a degradation of the focus quality at the fiber entrance at maximum energy, indicating negligible effects on the wave front upon propagation in ambient air.

Concerning (i), the nonlinearities in the BBO amplification crystal, we point out that the energy adjustment of the final OPA stage output was carried out by varying the pump pulse energy of the TiSa by rotating its polarization with a half wave plate in combination with a polarizer, as shown in Fig. 1. Since this is done before the compressor, there is no influence on other pump pulse properties by this method. On the other hand, the amplification conditions might change as a function of pump intensity. Therefore, we monitored the pulse duration as a function of pump energy and observed a pulse shortening towards higher energies from 50 fs in the unpumped case down to 40 fs at maximum intensity.[30] The on-axis B-integral of the 800 nm pump beam in the 2 mm

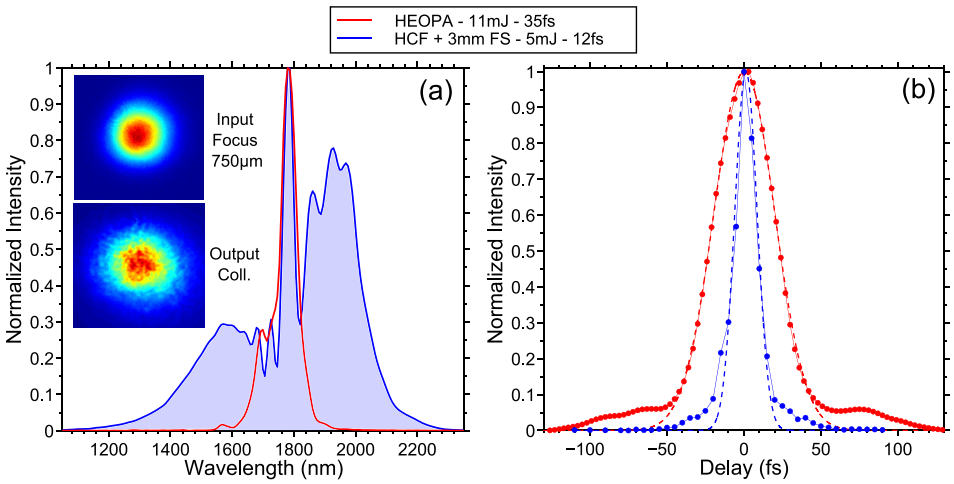

FIG. 3. Characterization of the fiber input and output pulses. (a) Spectrum of the multi-cycle input pulse in red compared with the broad spectrum at a pressure 300 mTorr at the exit side in shaded blue. Inset: CCD images of the input pulse focal spot (up) and of the output pulse collimated at 2 m after the fiber. (b) Autocorrelation trace of the multi-cycle input pulse in red and of the compressed 2-cycle pulse. Dotted lines denote a Gaussian fit.

thick BBO (extraordinary axis) is calculated to be 0.5 rad. As mentioned previously, the focal spot quality did not change and the 20% change in pulse duration would not explain a significant drop of fiber transmission. The next possibility (ii), nonlinearities in the vacuum window or beam splitters, seems less likely since the total on axis B-integral is estimated to be less than about 1 rad. The low average power of only 1 W is not expected to cause any thermal effect. Compared with this, the most strained optic is the last folding mirror of the input telescope, as shown in Figure 1. We estimated the on axis peak intensity to go beyond 10 TW/cm^2. This high intensity is caused by the fact that we had to build a compact telescope due to space restrictions. A very recent publication reports reversible, nonlinear absorption effects in dielectric mirrors already at much lower intensities for fs pulses, see cf. Fig. 2 in Ref. 38. In their study, they report on a dramatic reflectivity drop from 100% down to 20% at elevated intensities. Since we observed a similar reversible effect, this nonlinear absorption is currently our prime suspect to explain our observation.

In conclusion, improving upon the design of the stretched flexible hollow-core fiber scheme, we demonstrated pulse compression to 2-cycles (12 fs) at 1.8 μm wavelength with an energy of 5 mJ at 100 Hz repetition rate. The clean spatial profile together with a to date unmatched pulse power of 0.42 TW make it a very promising source for a large variety of strong field driven experiments like generation of high harmonics and high-field THz pulses. Further energy scaling seems feasible when using He or Ne as the nonlinear medium instead of Ar, or by employing circularly polarized pulses.[39]

The authors wish to acknowledge research funding from NSERC (Natural Sciences and Engineering Research Council of Canada), FRQNT (Fonds de recherche du Québec—Nature et technologies), Canada Foundation for Innovation—Major Science Initiatives, NanoQuébec, Ministère du développement économique, de l'Innovation et de l'exportation (MDEIE) du Québec, and DARPA PULSE Program through a Grant from AMRDEC. V.C., S.B., and V.W. express their gratitude for the scholarships awarded by NSERC. All authors are grateful for the efficient and dedicated work done by Antoine Laramée and Philippe Lassonde in ALLS.

[1]D. Strickland and G. Mourou, Opt. Commun. **55**, 447 (1985).
[2]D. Herrmann, L. Veisz, R. Tautz, F. Tavella, K. Schmid, V. Pervak, and F. Krausz, Opt. Lett. **34**, 2459 (2009).
[3]S. Witte and K. S. E. Eikema, IEEE J. Sel. Top. Quantum Electron. **18**, 296 (2012).
[4]D. Brida, G. Cirmi, C. Manzoni, S. Bonora, P. Villoresi, S. De Silvestri, and G. Cerullo, Opt. Lett. **33**, 741 (2008).
[5]Y. Deng, A. Schwarz, H. Fattahi, M. Ueffing, X. Gu, M. Ossiander, T. Metzger, V. Pervak, H. Ishizuki, T. Taira, T. Kobayashi, G. Marcus, F. Krausz, R. Kienberger, and N. Karpowicz, Opt. Lett. **37**, 4973 (2012).
[6]N. Ishii, K. Kaneshima, K. Kitano, T. Kanai, S. Watanabe, and J. Itatani, Opt. Lett. **37**, 4182 (2012).
[7]B. E. Schmidt, N. Thiré, M. Boivin, A. Laramée, F. Poitras, G. Lebrun, T. Ozaki, H. Ibrahim, and F. Légaré, Nat. Commun. **5**, 3643 (2014).
[8]A. Braun, G. Korn, X. Liu, D. Du, J. Squier, and G. Mourou, Opt. Lett. **20**, 73 (1995).
[9]G. Stibenz, N. Zhavoronkov, and G. Steinmeyer, Opt. Lett. **31**, 274 (2006).
[10]C. Hauri, A. Guandalini, P. Eckle, W. Kornelis, J. Biegert, and U. Keller, Opt. Express **13**, 7541 (2005).
[11]A. J. Verhoef, A. V. Mitrofanov, E. E. Serebryannikov, D. V. Kartashov, A. M. Zheltikov, and A. Baltuška, Phys. Rev. Lett. **104**, 163904 (2010).
[12]M. Nisoli, S. De Silvestri, and O. Svelto, Appl. Phys. Lett. **68**, 2793 (1996).
[13]Y. Matsuura, T. Oyama, and M. Miyagi, Appl. Opt. **44**, 6193 (2005).
[14]X. Jiang, D. Chen, and G. Hu, Appl. Opt. **52**, 770 (2013).
[15]P. S. J. Russell, J. Lightwave Technol. **24**, 4729 (2006).
[16]C. F. Dutin, A. Dubrouil, S. Petit, E. Mével, E. Constant, and D. Descamps, Opt. Lett. **35**, 253 (2010).
[17]J. Rothhardt, S. Hädrich, A. Klenke, S. Demmler, A. Hoffmann, T. Gottschall, T. Eidam, M. Krebs, J. Limpert, and A. Tünnermann, Opt. Lett. **39**, 5224 (2014).
[18]M. Nurhuda, A. Suda, K. Midorikawa, M. Hatayama, and K. Nagasaka, J. Opt. Soc. Am. B **20**, 2002 (2003).
[19]S. Bohman, A. Suda, T. Kanai, S. Yamaguchi, and K. Midorikawa, Opt. Lett. **35**, 1887 (2010).
[20]W. Ettoumi, Y. Petit, J. Kasparian, and J.-P. Wolf, Opt. Express **18**, 6613 (2010).
[21]D. Wang, Y. Leng, and Z. Xu, Appl. Phys. B **111**, 447 (2013).
[22]G. Andriukaitis, D. Kartashov, D. Lorenc, A. Pugžlys, A. Baltuška, L. Giniūnas, R. Danielius, J. Limpert, T. Clausnitzer, E.-B. Kley, A. Voronin, and A. Zheltikov, Opt. Lett. **36**, 1914 (2011).
[23]G. Fibich and A. L. Gaeta, Opt. Lett. **25**, 335 (2000).
[24]S. Bohman, A. Suda, M. Kaku, M. Nurhuda, T. Kanai, S. Yamaguchi, and K. Midorikawa, Opt. Express **16**, 10684 (2008).
[25]M. Nisoli, S. De Silvestri, O. Svelto, R. Szipöcs, K. Ferencz, C. Spielmann, S. Sartania, and F. Krausz, Opt. Lett. **22**, 522 (1997).
[26]B. E. Schmidt, P. Bejot, M. Giguère, A. D. Shiner, C. Trallero-Herrero, E. Bisson, J. Kasparian, J.-P. Wolf, D. M. Villeneuve, J.-C. Kieffer, P. B. Corkum, and F. Légaré, Appl. Phys. Lett. **96**, 121109 (2010).
[27]B. E. Schmidt, A. D. Shiner, P. Lassonde, J.-C. Kieffer, P. B. Corkum, D. M. Villeneuve, and F. Légaré, Opt. Express **19**, 6858 (2011).
[28]T. Nagy, M. Forster, and P. Simon, Appl. Opt. **47**, 3264 (2008).
[29]T. Nagy, V. Pervak, and P. Simon, Opt. Lett. **36**, 4422 (2011).
[30]N. Thiré, S. Beaulieu, V. Cardin, A. Laramée, V. Wanie, B. E. Schmidt, and F. Légaré, Appl. Phys. Lett. **106**, 091110 (2015).
[31]A. Suda, M. Hatayama, K. Nagasaka, and K. Midorikawa, Appl. Phys. Lett. **86**, 111116 (2005).
[32]E. Marcatili and R. Schmeltzer, Bell Syst. Tech. J. **43**, 1783 (1964).
[33]R. Abrams, IEEE J. Quantum Electron. **8**, 838 (1972).
[34]J. P. Crenn, Appl. Opt. **22**, 1426 (1983).
[35]P. Béjot, B. E. Schmidt, J. Kasparian, J.-P. Wolf, and F. Legaré, Phys. Rev. A **81**, 63828 (2010).
[36]D. Anderson and M. Lisak, Phys. Rev. A **27**, 1393 (1983).
[37]A. Gaeta, Phys. Rev. Lett. **84**, 3582 (2000).
[38]O. Razskazovskaya, T. Luu, M. Trubetskov, E. Goulielmakis, and V. Pervak, Optica **2**, 803 (2015).
[39]X. Chen, A. Jullien, A. Malvache, L. Canova, A. Borot, A. Trisorio, C. G. Durfee, and R. Lopez-Martens, Opt. Lett. **34**, 1588 (2009).